Neutron Activation and Shielding of the Light Ion Fusion Target Development Facility

K.J. O'Brien, G.A. Moses, and A.M. White

May 1983

UWFDM-512

Presented at the Fifth ANS Topical Meeting on the Technology of Fusion Energy, 26-28 April 1983, Knoxville, TN; Nucl. Tech./Fusion 4, 883 (1983).

Neutron Activation and Shielding of the Light Ion Fusion Target Development Facility

K.J. O'Brien, G.A. Moses, and A.M. White

Fusion Technology Institute
University of Wisconsin
1500 Engineering Drive
Madison, WI 53706

http://fti.neep.wisc.edu

May 1983

UWFDM-512

Presented at the Fifth ANS Topical Meeting on the Technology of Fusion Energy, 26-28 April 1983, Knoxville, TN; Nucl. Tech./Fusion 4, 883 (1983).

NEUTRON ACTIVATION AND SHIELDING OF THE LIGHT ION FUSION TARGET DEVELOPMENT FACILITY

K.J. O'BRIEN, University of Wisconsin
Nuclear Engineering Department
1500 Johnson Drive
Madison, Wisconsin 53706
(608) 263-3368

G.A. MOSES, A.M. WHITE, University of Wisconsin
Nuclear Engineering Department
1500 Johnson Street
Madison, Wisconsin 53706
(608) 263-3368

ABSTRACT

It has been proposed to surround the target chamber of the Light Ion Fusion Target Development Facility with a water shield. Such a shield would effectively isolate the radioactive chamber from the environment while providing a medium in which to absorb energy imparted to the target chamber walls following the impact of the fireball. Radioactivity calculations will be presented for five different wall materials.

If the water surrounding the chamber provides a damping mechanism for the wall vibrations, it also provides a medium through which a pressure pulse can be transmitted to the outer wall of the shield region. It is desirable to minimize the pressure loading upon this structure.

An investigation of the effects of a bubble screen upon the propagation of the water pressure wave is presented, along with some possible criteria for the design of a screen.

INTRODUCTION

The Target Development Facility,[1] Fig. 1, is an experimental facility that operates in an environment that includes a copious number of high energy neutrons. These neutrons will, of course, activate the structures surrounding the exploding target and will pose a direct radiological hazard to operating personnel if they are not shielded. Furthermore, the operating personnel must be shielded from the decay radiation from the activated components. Because this is an experimental facility easy access to it will be of utmost importance. This last constraint leads to a design that utilizes low activation materials and an easily removable shield. In this paper we first look at the problem of neutron activation and then give the details about the design of a water shield.

NEUTRON ACTIVATION

An investigation of five candidate materials for the first wall and structure shows that each is acceptable for the first wall structure if only mechanical and thermal response to the target explosion are considered.[2] However, their neutron activation properties are considerably different. Neutron transport calculations using the one-dimensional ANISN code were done using a neutron spectrum that was assumed to be softened by interactions in the compressed target. For this steady state calculation it was assumed that the fusion power was 23 kW (200 MJ yield at 10/day). With 70% of the energy in neutrons, this gives a neutron power of 16 kW and a neutron loading of 1.4×10^{-4} MW/m^2. At this wall loading materials damage will not be a serious consideration.

Neutron fluxes at the first wall were used to compute the activity of the first wall and the dose level experienced at the first wall. The total activity as a function of time is shown in Fig. 2 for Al 6061. This activity assumes a one year operating time at 23 kW of fusion power. This activity represents less than 100 curies at 10 years after shutdown. However, the important consideration is the dose received by personnel servicing the target chamber. This is given in Table 1 for the five candidate materials. The dose received at the first wall surface and 8 m from the first wall, on the operating floor, are both given. At shutdown, the aluminum has the highest dose. This quickly decays in a week to very low levels, 1.65 mr/hr, at the first wall surface. The Cu-Be alloy has a similar characteristic but does not decay as rapidly. The steels and Ti alloy have substantial dose rates on the order of 100 mr/hr at one week after shutdown. Only the Al 6061 and Cu-Be will allow extended hands-on servicing within the target chamber. The steels and Ti will allow limited hands-on maintenance or remote maintenance from the operating floor.

SHIELD ACOUSTIC WAVE ANALYSIS

For the purposes of this study the target

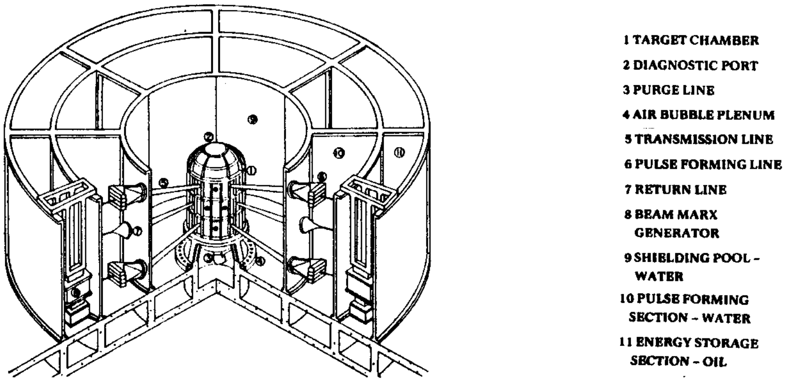

Fig. 1. Light Ion Fusion Target Development Facility.

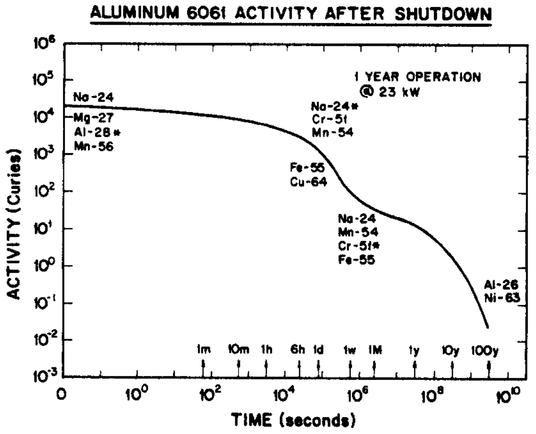

Fig. 2. Activation of first wall in TDF.

chamber will be modeled as a single component, of uniform composition, comprised of a cylindrical barrel with hemispherical caps. This vessel will pulsate harmonically. Transient effects will be ignored; the wall begins damped oscillations at time zero with maximum velocity taken at this time. This has no effect upon further analysis except to eliminate the transient wavefront emitted by the vessel during this time.

The acoustic wave analysis begins with a nonlinear treatment of the fluid dynamics, allowing the possibility of shocks.[3] The equations are then specialized to the linear acoustic case for the remainder of the analysis.

TABLE 1. Dose Calculations for LIB-TDF

One Year Operating Time at 23 kW

Dose at First Wall (mr/hr)

Material	Time After Shutdown 0	 1 day	 1 week
Al 6061	2,100	260	1.65
HT-9	489	114	101
304 SS	481	109	105
Ti-6Al-4V	515	177	66
Cu-Be	1,060	204	7

Dose at Operating Floor (mr/hr)

Material	Time After Shutdown 0	 1 day	 1 week
Al 6061	230	28	0.18
HT-9	55	13	11
304 SS	54	12	12
Ti-6Al-4V	59	20	7.5
Cu-Be	118	22	0.82

Neglecting the stresses due to viscosity and assuming only radial dependence the Navier-Stokes equation reduces to:

$$\rho(r,t)\,\frac{\partial V}{\partial t}(r,t) + \rho(r,t)V(r,t)\,\frac{\partial V}{\partial r}(r,t) = \frac{\partial}{\partial r}P(r,t)$$

$$\frac{\partial}{\partial t} \rho(r,t) + \frac{1}{r^k} \frac{\partial}{\partial r} \left(\rho(r,t)V(r,t)r^k\right) = 0.$$

where: ρ = density
V = velocity
P = pressure, and
k = 1,2 for cylindrical or spherical geometry.

With the introduction of a velocity potential this equation reduces to a non-linear wave equation:

$$V(r,t) = \frac{\partial}{\partial r} \phi(r,t)$$

$$\nabla^2 \phi - \frac{1}{c^2} \frac{\partial^2 \phi}{\partial t^2} = \frac{1}{c^2} \left(\frac{\vec{V}}{2} \cdot \vec{\nabla}\vec{V}^2 - \frac{d}{dt} V^2\right) .$$

The solution of the linearized form of this wave equation in spherical geometry is

$$P(r,t) = \frac{\rho_o V_w}{\left(1 - r^2 \frac{\omega^2}{c^2}\right)\left(\omega^2 + \left(\frac{c}{R_w} - \gamma\right)^2\right)} \frac{R_w}{r}$$

$$\left[\left(A\cos \omega\left(t - \frac{r - R_w}{c}\right)\right.\right.$$

$$\left.+ B\sin \omega\left(t - \frac{r - R_w}{C}\right)\right)e^{-\gamma\left(t- \frac{r-R_w}{c}\right)}$$

$$\left. + Ce^{-\frac{c}{R_w}\left(t- \frac{r - R_w}{c}\right)}\right]$$

where

$$A = r^2\omega^2\left(\frac{\omega^2 + \gamma^2}{c} - \frac{\partial\gamma}{R_w}\right)$$

$$+ r\left(\frac{c\gamma^2}{R_w} - \gamma(\gamma^2 + \omega^2)\right) + \left(c(\gamma^2 + \omega^2) - \frac{c^2\gamma}{R_w}\right)$$

$$B = r^2\left(\frac{\omega\gamma}{c} (\gamma^2 + \omega^2)\right.$$

$$\left.+ \frac{\omega}{R_w} (\omega^2 - \gamma^2)\right) + r\left(- \frac{\omega c\gamma}{R_w}\right) + \frac{\omega c^2}{R_w}$$

$$C = r^2\left(\frac{\omega^2 c}{R^2}\right) + r\left(c \frac{\gamma^2 + \omega^2}{R_w} - \frac{c^2\gamma}{R_w} - \frac{\omega^2 c}{R_w}\right)$$

$$+ \left(\frac{c^2\gamma}{R_w} - (\gamma^2 + \omega^2)c\right) .$$

This function is depicted in Fig. 3. All physical parameters and design parameters are given in Table 2. Figure 3 depicts the wave fronts for times 0.1 to 0.7 ms. The wave fronts end abruptly since the motion of the wall is assumed to begin at time zero at maximum velocity on the expansion cycle. The detailed structure of the wave front beyond the abrupt termination depends upon the initial movements of the wall during the transient period. The pressure amplitude at the outer wall as the waves reach it is given in Fig. 4. Similar results can be obtained for the cylindrical case.[3]

BUBBLE SCREENS

It is of interest to contemplate the use of a screen of small bubbles as a barrier to and absorber of the pressure waves launched by the TDF target chamber. Although many of the models employed are perhaps oversimplifications it is hoped that the major issues involved are clearly delineated. Further work could be carried out to improve the details of the analysis. The pronounced effect of gas bubbles in a fluid upon the sound propagation within that fluid is well known. A few widely dispersed bubbles, so small as to be invisible, have an appreciable acoustic effect. The propagation speed is greatly diminished and substantial attenuation occurs. Fluids containing a large number of bubbles will be practically opaque to acoustic waves.

"Bubbles excited to volume pulsations have a polytropic equation of state for the enclosed gas which results in a phase difference between the change in pressure per unit original pressure and the change in volume per unit original volume. Therefore, the work done in compressing the bubble is more than the work done

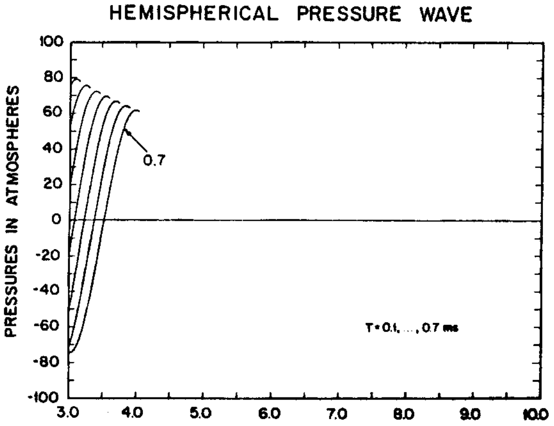

Fig. 3. Acoustic waves in water shield.

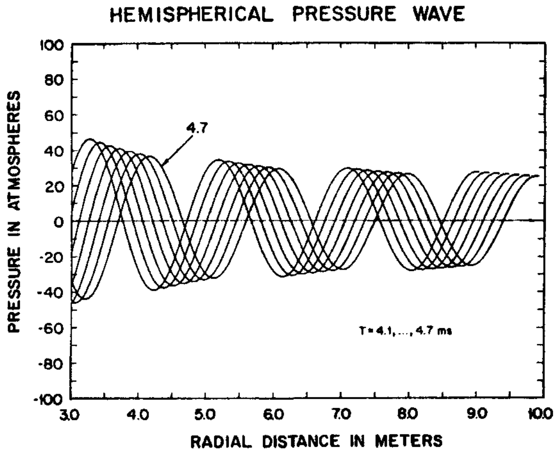

Fig. 4. Pressure at outer boundary of water shield.

TABLE 2. SPECIFIC PARAMETERS FOR ACOUSTIC WAVE AND BUBBLE SCREEN CALCULATIONS

Target Chamber Parameters

R_W = 3 m barrel and hemisphere radius
H_W = 6 m barrel height
ω = 4838 s^{-1} vibration angular frequency
V_W = 5.7 m/s maximum wall velocity
E = 60 MJ blast wave hydrodynamic energy per shot
γ = 0.118 ms^{-1} damping constant

Fluid Physical Data

ρ_o = 10^3 kg/m^3 water density
c = 1470 m/s sound speed
κ_W = $4.76 \ast 10^{-10}$ m^2/nt compressibility

Bubble Physical Data

R_o = 4 mm resonant bubble radius
R_b = 2 mm bubble radius
δ_o = 0.02 bubble resonant damping constant
σ = 0.07 J/m^2 bubble surface tension
κ_b = $5 \ast 10^{-6}$ m^2/nt compressibility

by the bubble in expanding; this difference in the work done represents a net flow of energy into the liquid."(4) The damping associated with this mechanism is called thermal damping.

A second damping mechanism is called radiation damping. Pulsating bubbles act as sources of outgoing spherical sound waves. A fraction of the bubble energy is radiated in this fashion. Since this energy is initially in the incident or driving wave this represents a loss mechanism for the incident wave mode. The combined effect of many such oscillating bubbles is a randomization of the wave energy initially organized in the incident wave.

The third important damping effect is that of viscosity. Although as a bulk the fluid is considered to be inviscid, at the fluid-gas interface viscous forces are included. As the bubble rapidly expands and contracts this viscous effect results in heating of the fluid.

The possibility of bubble breakup and the associated energetics of the latent heat of surface formation will not be considered. The bubbles are small enough that breakup seems unlikely.

A total damping constant is defined to be the reciprocal of the Q-value of the bubble-fluid system. The Q-value characterizes the fraction of remaining energy lost per cycle. In terms of the three mechanisms discussed, the total damping is

$$\delta = \delta_{rad} + \delta_{th} + \delta_{vis} .$$

A general theory of scattering from randomly distributed scatterers is applied in Ref. (5) to derive the attenuation in decibels of a wave incident upon a bubble screen. For normal incidence the result is

$$K = 4.34 \frac{4\pi R \frac{R_o^3}{R^3} \delta_o \frac{\omega}{c}}{\left(\frac{R_o^2}{R^2} - 1\right)^2 + \frac{R_o^6}{R^6} \delta_o^2} ns$$

n = bubble number density
R = bubble radius
R_o = resonant bubble radius
s = screen thickness
δ_o = resonant damping constant.

From this, an exponential damping coefficient can be computed as

$$\alpha = 3 \frac{c}{\omega} \delta_o x \frac{1}{R_o^2} \left[\frac{\xi^5}{(1 - \xi^2)^2 + \xi^6 \delta_o^2}\right] .$$

where $\xi = R_o/R$.

To analyze the effect of a bubble screen in the TDF shield pool we assume that acoustic waves are normally incident upon a homogeneous slab of bubbles dispersed within a fluid. The acoustic properties within the slab are characterized by a sound speed c_2 and attenuation coefficient α. Outside the screen the sound speed is c_1 and there is no attenuation.

Reflected pressure amplitudes are depicted in Fig. 5 for screen widths between 0.1 and 0.4 meters using a bubble radius of 2 mm, which is half the resonant radius. This figure shows that appreciable reflection occurs. This situation seems undesirable since the reflected waves are focused back upon the pulsating vessel. However, an appropriate choice of screen thickness and void fraction gives a screen with a tolerable reflection ratio. This situation represents a "tuned screen" which effectively divides the waves into acceptable reflected and transmitted components.

Figures 6-8 depict the absorption, transmission, and reflection power ratios respectively for a screen of width 0.4 m with void fraction x = 0.00075. These results show a favorable rate of energy absorption while the reflection is tolerable.

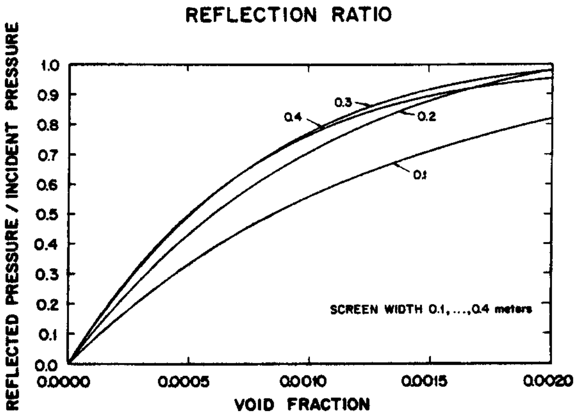

Fig. 5. Reflection ratio of acoustic waves from bubble shield.

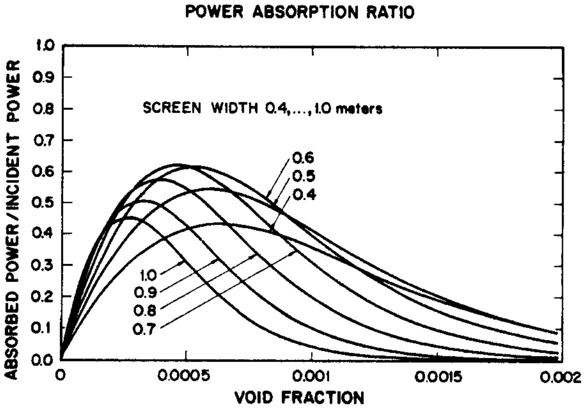

Fig. 6. Absorption of acoustic wave in bubble screen.

CONCLUSIONS

A water shield for the LIF-TDF allows easy access to the target chamber. This is very important for such an experimental facility. The use of low activation materials, like Al 6061, for the first wall and structure allows hands on maintenance within the target chamber one week

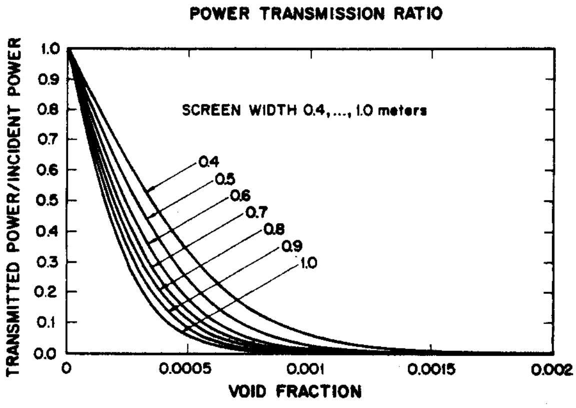

Fig. 7. Transmission of acoustic wave through bubble screen.

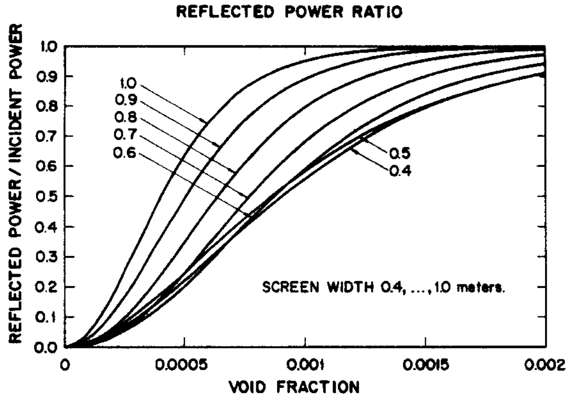

Fig. 8. Reflection of acoustic wave from bubble screen.

after shutdown. The careful design of a bubble screen effectively attenuates acoustic waves launched into the water shield by the pulsating target chamber.

ACKNOWLEDGMENT

This work was supported by Sandia National Laboratory under contract number DE-AS08-81DP40161.

REFERENCES

1. G.A. MOSES, R.R. PETERSON, R.L. ENGELSTAD, E.G. LOVELL, G.L. KULCINSKI, K.J. O'BRIEN, A.M. WHITE, and J.J. WATROUS, "Light Ion Fusion Target Development Facility Pre-Conceptual Design", *Proc. 5th ANS Topical Mtg. on Tech. of Fusion Energy.*

2. R.R. PETERSON, E.G. LOVELL, R.L. ENGELSTAD, G.L. KULCINSKI, G.A. MOSES, K.J. LEE, "First Wall Materials Selection in the Light Ion Beam Target Development Facility" *Proc. 5th ANS Topical Mtg. on Tech. of Fusion Energy.*

3. K.J. O'BRIEN, G.A. MOSES, "Bubble Screen Shielding of Water Pressure Waves Emitted by a Harmonically Pulsating Vessel," University of Wisconsin Fusion Engineering Program Report UWFDM-476 (July 1982).

4. C. DEVIN, "Survey of Thermal, Radiation and Viscous Damping of Pulsating Air Bubbles in Water," *J. Acoust. Soc. Am., 31,* 1654-1667 (1959).

5. E.L. CARSTENSEN, L.L. FOLDY, "Propagation of Sound Through a Liquid Containing Bubbles," *J. Acoust. Soc. Am., 19,* 481-501 (1947).